

# **NATURAL FIELD INDUCED POLARIZATION FOR MAPPING OF DEEP MINERAL DEPOSITS: A CASE STUDY FROM ARIZONA**

**Erika Gasperikova<sup>1</sup>, Nestor Cuevas<sup>2</sup>, and H. Frank Morrison<sup>3</sup>**

<sup>1</sup>Lawrence Berkeley National Laboratory, 1 Cyclotron Road, MS: 90R1116, Berkeley, CA 94720  
email: egasperikova@lbl.gov

<sup>2</sup>Electromagnetic Instruments Inc.

<sup>3</sup>University of California, Berkeley

Submitted: April 10, 2003

## **ABSTRACT**

This paper describes a case study of the natural field induced polarization (NFIP) method over a known deep induced polarization (IP) target in Arizona. Data processing and interpretation were successful in extracting the IP target from the natural field signals in the presence of a conductive shallow surface layer. The extracted target correlated well with an earlier IP/resistivity dipole-dipole survey. So far, the NFIP method shows excellent potential as a commercial survey technique for the mineral industry. It eliminates the expense and energy requirements of deploying large transmitters and is sensitive to deeper structures (structures than cannot be resolved using traditional methods).

## INTRODUCTION

The frequency dependent resistivity phenomenon, known as induced polarization (IP), reflects the degree to which the subsurface is able to store electrical charge. This phenomenon is associated with disseminated metallic deposits, such as porphyry copper deposits, and is exploited by resistivity surveys to detect IP targets. Standard field techniques for mapping IP rely on the use of grounded electrodes, most commonly in the dipole-dipole or pole-dipole configuration. After current is introduced into the ground through two current electrodes, the potential difference is measured between two potential electrodes located at some distance from the current electrodes. In the frequency domain, the apparent resistivity, or the impedance phase, is measured at frequencies low enough such that any electromagnetic (EM) coupling is either negligible or predictable. EM coupling increases with the receiving dipole length and dipole separation, as well as with conductivity and frequency (Dey and Morrison, 1973).

As the exploration depth increases, power requirements and measurement time increase dramatically, for two reasons. First, the dipoles and their electrode separation must be larger; hence, the operational frequency must be low to avoid EM coupling. Second, since the natural EM field spectrum rises steeply below 1.0 Hz, excessive power is required to achieve an adequate signal-to-noise ratio. The increasing natural field spectrum (which is noise in traditional IP surveys) is the desirable signal source in a natural field method. Natural field induced polarization (NFIP) is a method for detecting the IP response using naturally occurring magnetotelluric signals as the source, thereby removing the need for cumbersome and expensive transmitters.

The NFIP method was formulated by Gasperikova and Morrison (2001). This method makes it possible to extract the frequency dependence of a polarizable target when the target is responding at its DC limit. At a sufficiently low frequency, there is negligible induction, and the measured response is that of the body distorting the background currents. Profiles of low-frequency natural electric (telluric) fields have spatial anomalies over finite bodies of fixed conductivity that are independent of frequency and have no associated phase anomaly. If the body is polarizable, the electric field profile over the body becomes frequency-dependent and phase shifted with respect to a reference field. Target dimension and conductivity information is important for calculating a skin depth, which helps to define the frequency range and profile length necessary for recovering IP response from the data. The advantage of the NFIP method over conventional IP surveys is that it becomes more effective as the target depth increases, since the source signals also increase.

## **DATA ACQUISITION**

### **Survey Setup**

The NFIP survey was done along a 6.2 km long profile with 200 m site separation. The field setup consisted of two remote stations with orthogonal electric and magnetic sensors, and data along the profile were acquired with an L-shape configuration: two electric dipoles along the line and one electric dipole perpendicular to the line. A schematic of the setup is shown in Figure 1. The survey was done with seven

acquisition systems. Excellent-quality data were collected within 0.001–10 Hz band. In general, data recording time was at least 20 hours, with four or more systems acquiring data simultaneously most of the time.

Our MT survey was laid out along the line of the dipole-dipole IP/resistivity survey from 1975 (Andrews, 1975). The schematic geological cross section along this profile is shown in Figure 2. This profile traverses an area of thick Quaternary alluvium, Tertiary lake-bed sediments (Ts), and volcanics (Tv) overlying a possible sulfide system developed in Cretaceous andesites (Ka). These andesites were intruded upon by Laramide porphyry (TKg) in the form of north-trending dikes and possibly sills. The bedrock is relatively shallow on the right side of the profile, with the thickness of Tertiary sediments increasing to the left. A fault around the 0 m location (in Figure 2) cuts off these sediments against Tertiary volcanics and displaces andesites about 100 feet (30 m). Disseminated mineralization was intersected in a drill hole indicated on the profile as DH4, with the dotted line representing a base of oxidation. The cutoff to sulfides is unknown. Andesites contain about 2–5 vol. % of pyrite, while the densely dotted area on the left side of the fault contains about 5–10 vol. % of pyrite.

## **DATA PROCESSING AND INTERPRETATION**

### **Resistivity/IP inversion**

Kennecott Exploration ran a dipole-dipole IP/resistivity survey along this line in the 1970s. Resistivity and IP inversions of these data sets were performed by using an inversion algorithm by Oldenburg and Li (1994). Field and calculated resistivity data are shown in Figure 3a, while field and calculated chargeability data are shown in Figure 3b. The resistivity inversion and the IP inversion are shown in Figure 4, with the resistivity inversion clearly indicating the vertical contact around 0 m. High-resistivity structures appear on both sides of the contact, with 5 Ohm-m conductive layer (basin sedimentary layer) on the left side of the contact (west side of the profile), and a 10–20 Ohm-m layer on the right side of it. The basin sedimentary layer overlies the porphyry and andesite structure (100 Ohm-m). Below this 100 Ohm-m structure, resistivity decreases to 10 Ohm-m, which suggests that the andesite and porphyry are sitting on another sedimentary layer. The IP inversion clearly shows a 60 milliradian anomaly associated with the porphyry structure between –2,000 m and 0 m. No significant IP anomaly is associated with the structure on the right side of the contact.

### **MT Analysis**

Data were processed with a robust multistation processing program (Egbert, 1997). Some problems arose with data acquisition at stations 44W and 46W, and

therefore data from these locations were not used in the interpretation. In general, high-quality data were obtained in the frequency range between 0.001 Hz and 10 Hz. Figure 5a and 5b show TM-mode resistivity and phase cross sections, respectively, along the profile. Data were inverted with an algorithm by Rodi and Mackie (2001), and the resulting cross section (Figure 6) is in excellent agreement with the dipole-dipole inversion shown in Figure 4. The MT profile ran from –5,000 m to 1,200 m while the IP/resistivity profile ran from –2,500 m to 3,500 m. Apart from the contact around 0 m and a high resistivity porphyry structure (200 Ohm-m) around –1,000 m, MT inversion also recovers the full extent of andesites, which are slightly less resistive than the porphyry. Tertiary lake-bed sediments in the upper 300 m have a resistivity around 10–20 Ohm-m. Cretaceous andesites have resistivity around 100 Ohm-m and are about 1,000 m thick. The porphyry intruded into the volcanic sequence in the form of dikes ranging from a few tens to thousands of feet in width (Yarter, 1981). If the dikes were less than 1,000 feet (300 m) wide, our data would not be sensitive to them—this might be one of the reasons why we do not see the continuation of the porphyry structure through the deeper sediments. However, andesites clearly overlay deep conductive sediments, which suggests that the sulfides are not as deep as originally thought. The resistive basement (Paleozoic unit?) starts at a depth of 2,700 m. This is consistent with Yarter’s interpretation (1981) that “at least 3,000 feet (~1,000 m) of Cretaceous Mesozoic clastic rocks and interbedded volcanics separate Paleozoic carbonate units from the lower portions of the andesite.”

## NFIP Analysis

Following the procedure described by Gasperikova and Morrison (2001), we analyzed the change in the imaginary part of the ratio between local and reference fields. If the reference site electric field is  $Ae^{i(\omega t + \varphi_1)}$  and the electric field along the profile is  $Be^{i(\omega t + \varphi_2)}$ , then the ratio between these two fields can be expressed as  $\frac{B}{A}\cos(\varphi_2 - \varphi_1) + i\frac{B}{A}\sin(\varphi_2 - \varphi_1)$ . If the structure is at the static DC limit and no IP is present, no phase shift occurs between these two electric fields, and thus no imaginary component exists in the ratio. However, if the dipole along the profile traverses a body with IP,  $(\varphi_2 - \varphi_1)$  is non-zero, and therefore an imaginary component exists. Figure 7 shows the imaginary component of the impedance plotted for TM-mode ( $Z_{TM}$ ), normalized with the values from the area where no IP exists (right side of the profile). The plot shows that the porphyry structure around  $-1,000$  m, identified both by geology and by IP/resistivity inversion, was recovered. A similar response is seen around  $-2,000$  m and  $-3,000$  m. This response would suggest that other intrusions existed in the area apart from the one at  $-1,000$  m. Because the resistive structure to the right of the contact ( $+500$  m) has no imaginary component of  $Z_{TM}$  below  $0.1$  Hz, it is not a possible IP target. Thus, applying the procedure illustrated in Figure 7 to an area where we have no previous information, we can use the imaginary component of the normalized  $Z_{TM}$  as a mapping tool for identification of possible IP targets.

Data processing and interpretation were successful in extracting the IP target from natural field signals in the presence of a conductive shallow surface layer. The extracted IP response from the natural field data correlated well with a previous commercial DC resistivity and IP survey (Andrews, 1975).

## **CONCLUSIONS**

We have demonstrated in this MT survey that it is possible to extract IP information from magnetotelluric data. The NFIP method has excellent potential as a commercial survey technique for the mineral industry; further demonstrations over other types of IP targets are suggested. The advantages of this new field method are that: (1) it eliminates the expense and energy requirements of deploying large cumbersome transmitters, and (2) it is sensitive to deeper structures than can be resolved using traditional methods.

## **ACKNOWLEDGEMENTS**

This work was supported by U.S. Department of Energy under Contract No. DE-FC26-01NT41060. We thank Kennecott Exploration for making us aware of the site and for providing data from previous surveys.

## REFERENCES

- Andrews, R.K., 1975. The Sol sulfide system, Graham County, Arizona: Report on VIP work: Kennecott report, 17 p.
- Dey, A., and Morrison, H.F., 1973, Electromagnetic coupling in frequency and time-domain induced-polarization surveys over a multilayered earth: *Geophysics*, **38**, 380-405.
- Egbert, G.D., 1997, Robust multiple-station magnetotelluric data processing: *Geophysical Journal International*, **130**, 475-496.
- Gasperikova, E., and Morrison, H.F., 2001. Mapping of induced polarization using natural fields: *Geophysics*, **66**, 137-147.
- Oldenburg, D.W. and Li, Y., 1994, Inversion of induced polarization data: *Geophysics*, **59**, 1327-1341.
- Rodi, W., and Mackie, R.L., 2001, Nonlinear conjugate gradients algorithm for 2-D magnetotelluric inversion: *Geophysics*, **66**, 174-187.
- Yarter, W. V., 1981, Geology, geochemistry, alteration, and mass transfer in the Sol prospect, a sub-economic porphyry copper-molybdenum deposit, Safford District, Graham County, Arizona: MS Thesis, University of Arizona.

## LIST OF FIGURES

Fig. 1: Field Setup for MT24/LF systems showing E and H channel orientations.....	11
Fig. 2: Geologic cross section along the profile (after Andrews, 1975).....	12
Fig. 3a: DC resistivity inversion of dipole-dipole data: Observed and predicted data (data courtesy of Kennecott Exploration).....	13
Fig. 3b: IP inversion dipole-dipole data: Observed and predicted data (data courtesy of Kennecott Exploration).....	13
Fig. 4: DC resistivity and IP inversion of dipole-dipole data. ....	14
Fig. 5a: Apparent resistivity cross section for the TM mode.....	15
Fig. 6: MT inversion of TM data along the profile.....	16
Fig. 7: Cross section of the imaginary component of $Z_{TM}$ from NFIP survey, normalized by $Z_{TM}$ from the right end of the profile. ....	17

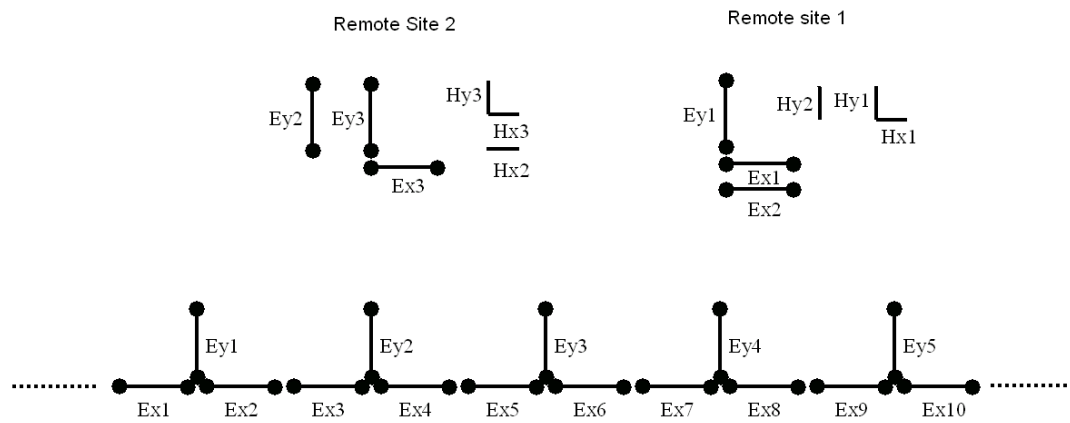


Fig. 1: Field Setup for MT24/LF systems showing E and H channel orientations.

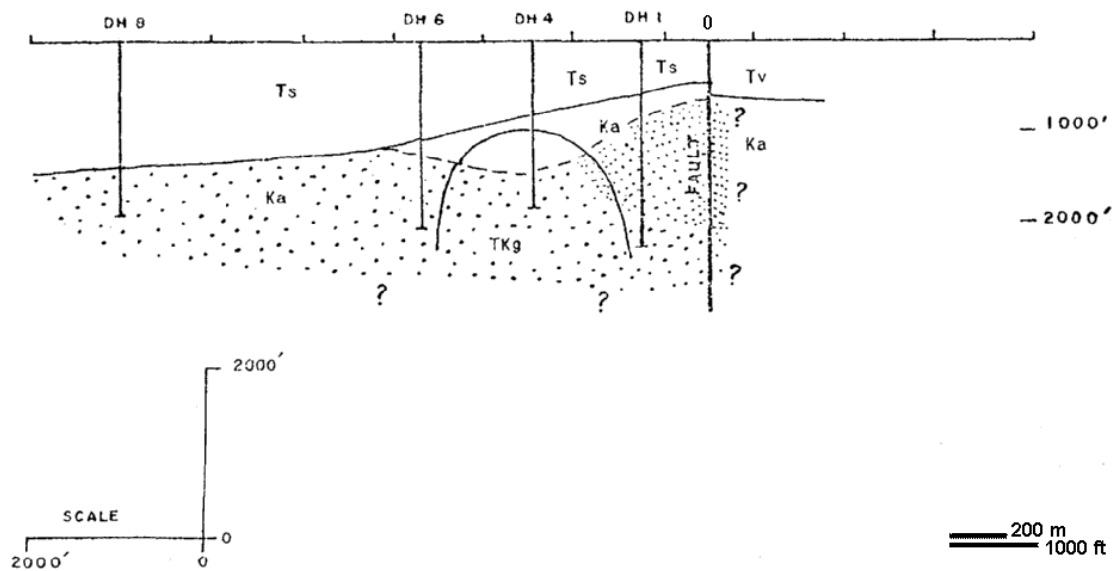


Fig. 2: Geologic cross section along the profile (after Andrews, 1975).

Gasperiikova et al., Figure 2

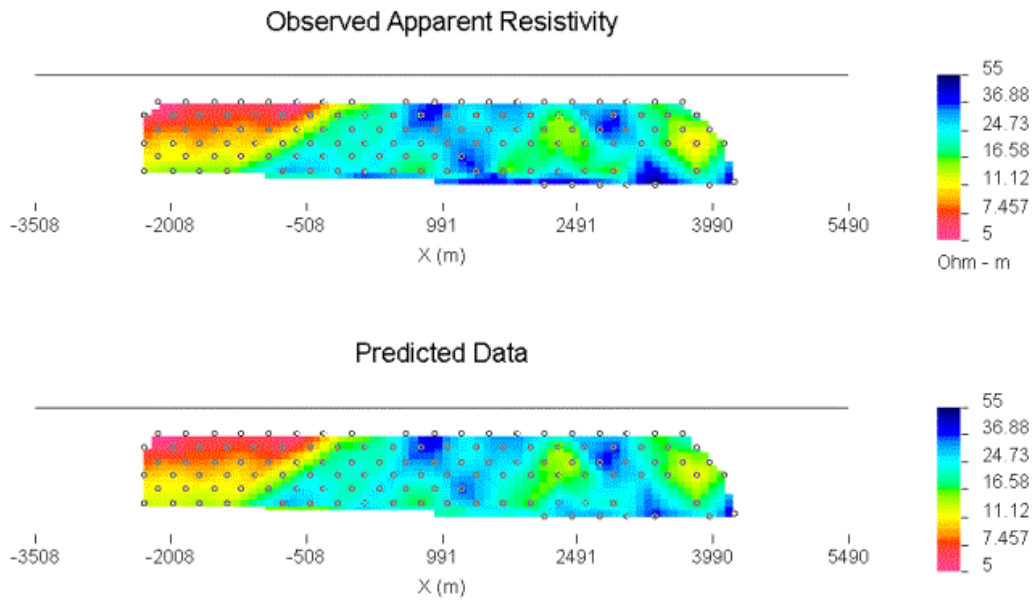


Fig. 3a: DC resistivity inversion of dipole-dipole data: Observed and predicted data (data courtesy of Kennecott Exploration).

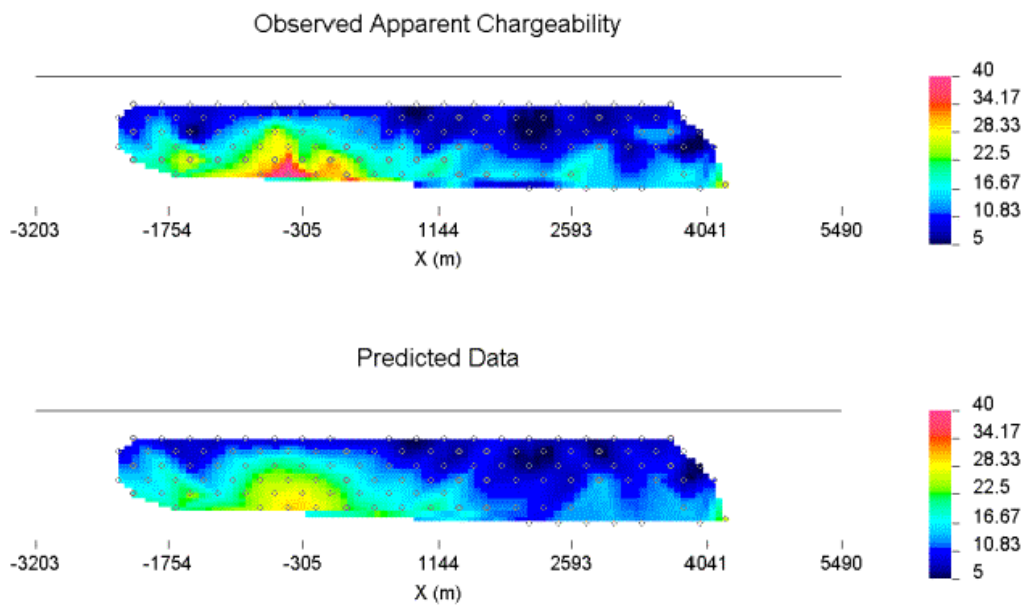


Fig. 3b: IP inversion dipole-dipole data: Observed and predicted data (data courtesy of Kennecott Exploration).

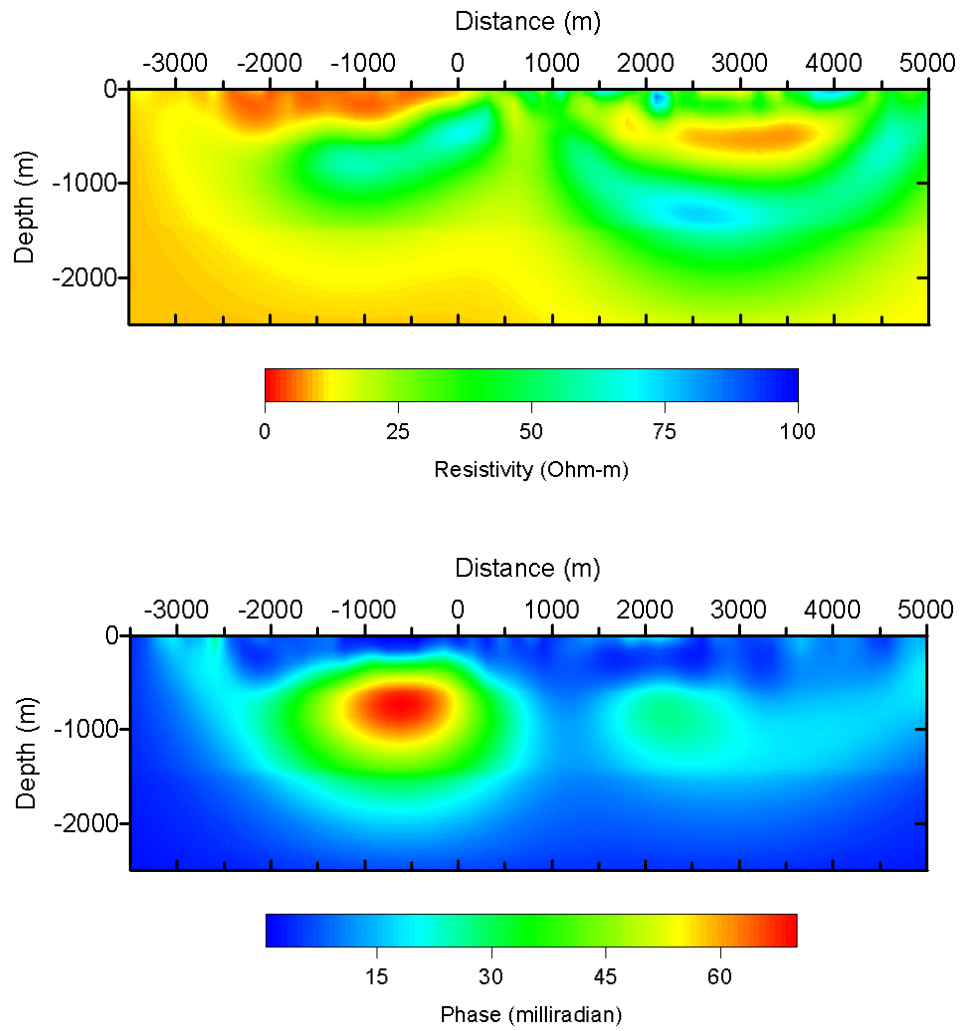


Fig. 4: DC resistivity and IP inversion of dipole-dipole data.

Gasparikova et al., Figure 4

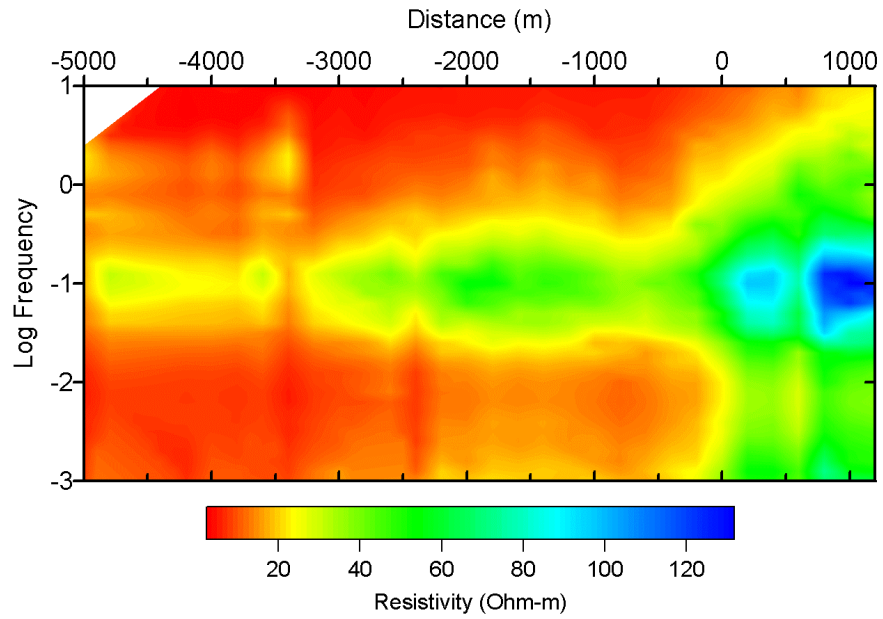


Fig. 5a: Apparent resistivity cross section for the TM mode.

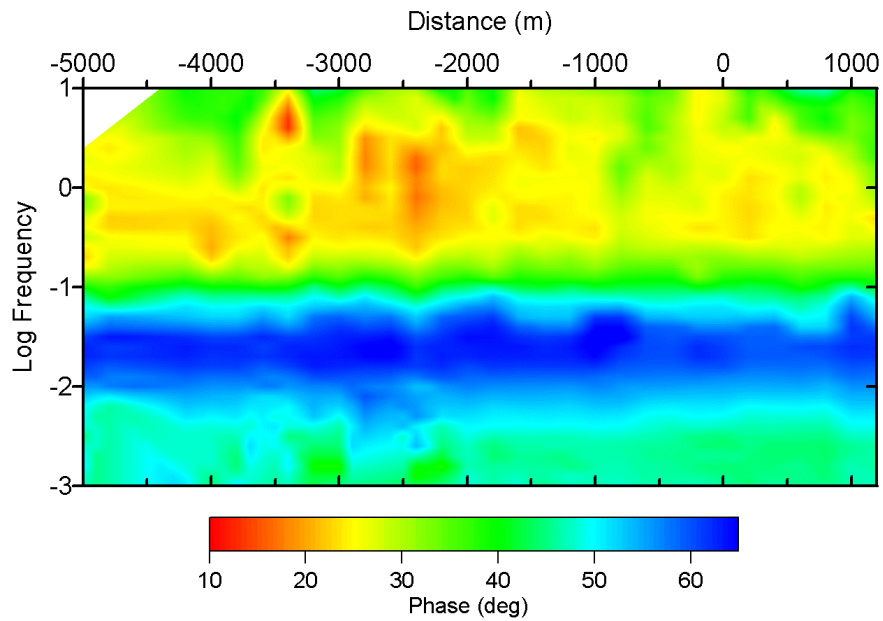


Fig. 5b: Phase cross section for the TM mode.

Gasparikova et al., Figure 5

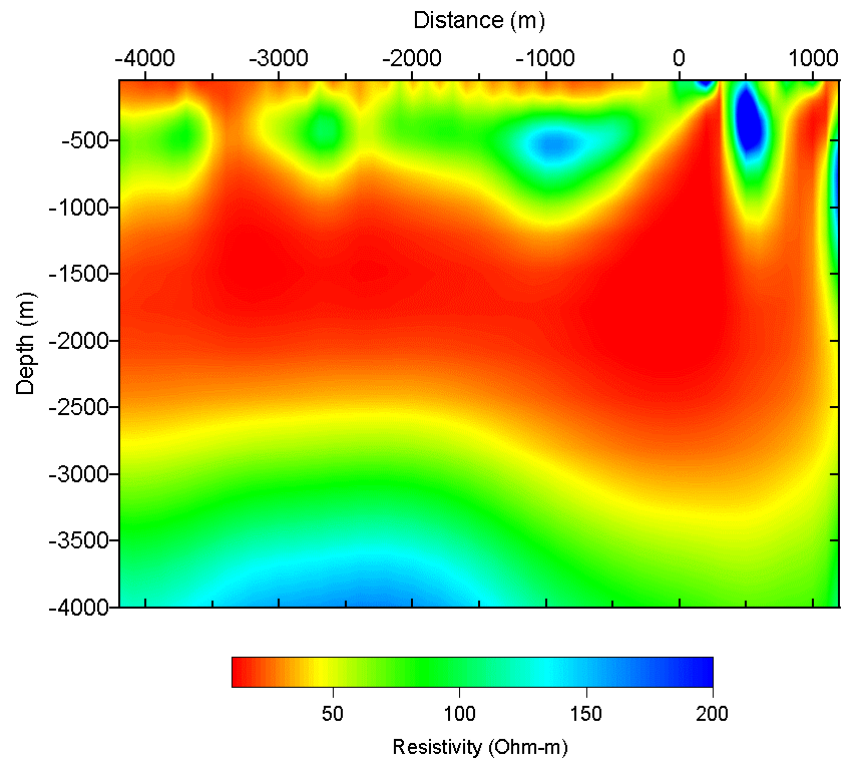


Fig. 6: MT inversion of TM data along the profile.

Gasperiikova et al., Figure 6

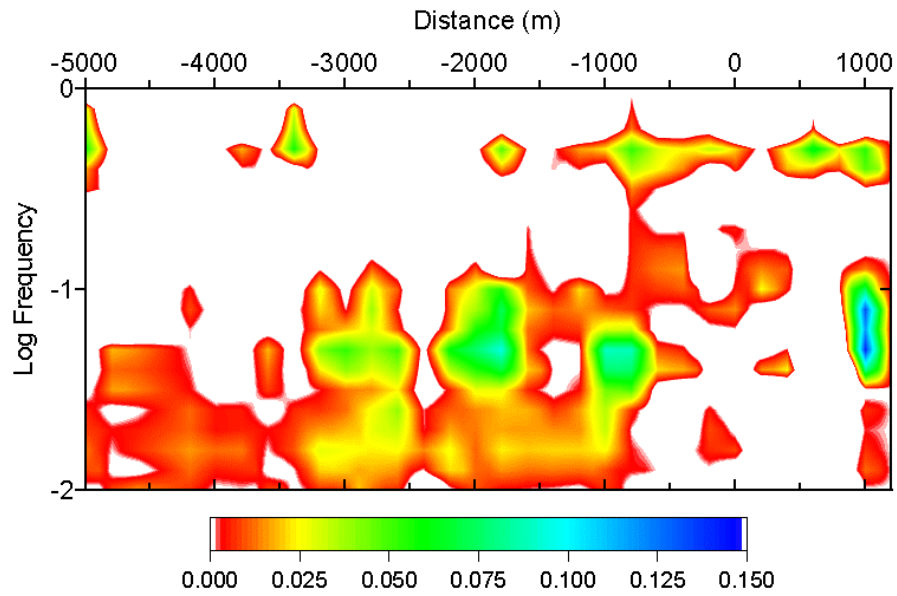


Fig. 7: Cross section of the imaginary component of  $Z_{TM}$  from NFIP survey, normalized by  $Z_{TM}$  from the right end of the profile.